RSC Advances

ROYAL SOCIETY OF CHEMISTRY

www.rsc.org/advances

Cite this: DOI: 10.1039/c0xx00000x

www.rsc.org/xxxxxx

COMMUNICATION

Photoelectrochemical activities and low content Nb doping effects on one-dimensional self-ordered Nb_2O_5-TiO_2 nanotubes

Linjuan Pei,[a] Min Yang,[*a] Dan Zhang,[a] Lei Zhang,[a] Peng Chen,[b] Yanyan Song,[c] and Yang Gan[a]

Received (in XXX, XXX) Xth XXXXXXXXX 2014, Accepted Xth XXXXXXXXX 2014

DOI: 10.1039/b000000x

Self-ordered Nb_2O_5-TiO_2 nanotube arrays were synthesized by anodization method from Ti-Nb alloy. Compared with pure TiO_2 nanotubes, Nb_2O_5-TiO_2 nanotubes shows enhanced surface hydrophilicity and low charge-transfer resistance. The beneficial Nb doping effects also exhibit in an improved separation efficiency, leading to higher photocatalytic and photoelectrocatalytic activities.

Introduction

At present, many research works have been devoted to one-dimensional self-ordered TiO_2 nanotubes since the first paper was published by Zwilling in 1999.[1] As an n-type functional semiconductor, due to good electrical transport property and large surface area TiO_2 nanotubes have succeeded in capturing the attentions and shown superior performances in applications of photocatalysis, dye-sensitized solar cells, electrochromic devices, batteries, supercapacitors, drug delivery and bioelectrochemical sensors.[2,3] For further modification of optical and electrical properties of TiO_2, a very wide range of elements (such as nonmetals N, C, B, S, P, F et al and transition-metal ions Cu, Co, Ni, Nb, Fe, Mo et al) were used in doping by intruding new band energy or localized states.[4,5] As a promising semiconductor material with band gap of about 3.4 eV, Niobium oxide (Nb_2O_5) has wide range of catalytic and photocatalytic activities, especially in selective oxidation of benzylamine.[6] In previous work,[7,8] different concentrations (from 0.05wt%~1wt%) of Nb_2O_5 doped TiO_2 nanotube were grown by electrochemical anodization method. By measuring the efficiency of dye-sensitized solar cell and photoresponse intensity, the optimal concentration was 0.1wt%.As reported, [9] an enhanced optical band-gap was found by heavily Nb_2O_5 doped TiO_2 (from 1% to 30%), which became a drawback for photoelectrochemical applications.

The Nb doping effect in solar cell is ascribed to the suppression of recombination of charge carriers. However, a limited amount of studies have involved in photocatalytic performance and Nb beneficial effects of Nb_2O_5-TiO_2 compounds. Only Cui et al had demonstrated submonolayer surface coverage and acidity were increased by introduction of 1.5-3mol% Nb_2O_5, which leaded to enhanced photocatalytic degradation of 1,4 dichlorobenzene.[10] As we known, photocatalytic process involves redox reaction happening at surface/interface of photocatalyst and solution. Besides the changes in surface properties with Nb doping, charge separation efficiency under light illumination also plays an important role in photocatalytic activity. Therefore, in this work we fabricate 0.1wt% Nb_2O_5 doped TiO_2 nanotube layers and focus on the Nb doping effects on surface wettability, charge-transfer resistance, surface energy band, behaviors of photogenerated carriers and corresponding results on photocatalytic activity.

Experimental

Nb_2O_5 doped TiO_2 nanotube arrays were prepared by anodization of 0.1wt% Ti-Nb alloy in glycerol (65vol%)-H_2O electrolyte containing 0.27 M NH_4F at 30 V for 3h. Tube fabrication was carried out in two-electrode system with Pt sheet as the counter. Pure TiO_2 nanotubes were grown in the same conditions as reference. All the samples were annealed at 450°C in air for 2h for crystallization.

The morphologies of samples were characterized by a field-emission scanning electron microscope (FE-SEM, Supra™55, Zeiss). X-ray diffractions analysis (XRD, D8-Advance, Bruker) with graphite monochromized $Cu_{K\alpha}$ radiation (λ=0.15406 nm) was collected for detecting the crystal structure of nanotubes. Surface hydrophilic properties were conducted on contact angle meter (SL200B, Suolun Ltd., China). All the electrochemical measurements were carried out by electrochemical station (CHI660D, ChenHua Ltd., China) with a Pt foil as the counter electrode and a Ag/AgCl electrode as the reference electrode. The surface contact potential difference (CPD) was obtained from a scanning Kelvin probe system (KP Technology Ltd., Scotland, UK). In Transient photovoltage (TPV) system, [11] samples were excited by a 50 μJ laser pulse (wavelength of 355 nm and pulse width of 5 ns) from a third-harmonic Nd:YAG laser (Polaris II, New Wave Research, Inc.). The TPV signals were recorded by a 500 MHz digital phosphor oscilloscope (TDS 5054, Tektronix). The surface photovoltage spectroscopy (SPV)[12] consists of a 500W xeon lamp (CHFXQ500W, Global xenon lamp power), a monochromator (SBP500, Zolix) and a lock-in amplifier (SR830-DSP, Standford) with an optical chopper (SR540, Standford) running at 23 Hz. The AC photovoltage signals were detected from a sandwich-like holder (Cu/sample/ITO) and were recorded as a function of wavelength. The photoelectrocatalytic measurement was performed in 0.1 M Na_2SO_4 with bias of +0.3V. As light sources, the monochromatic light of 365 nm with

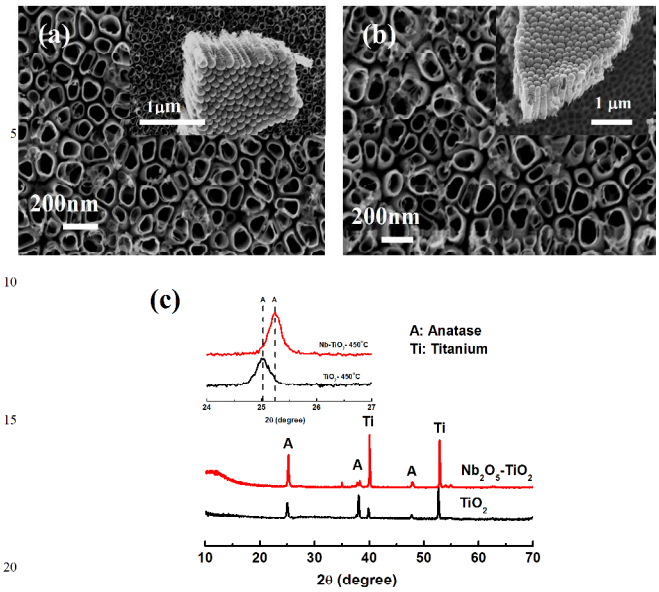

Fig.1 SEM images of TiO_2 nanotubes (a) and Nb_2O_5-TiO_2 nanotubes (b). Inset: cross-section images of nanotube layers. (c) XRD patterns of TiO_2 nanotubes and Nb_2O_5-TiO_2 nanotubes after annealing at 450°C. Inset of (c): magnified XRD patterns in the range of 2θ=24~27°

intensity of 5 mW/cm^2 was filtered from a 300 W Xe lamp (l300C, Perfect Light Ltd., China). For evaluation of photocatalytic activity, the concentration of an azo-dye (acid orange 7-AO7, $C_{16}H_{11}N_2O_4SNa$) with 1.5 × 10^{-5} mol/L was determined by periodically measuring the absorbance at 486 nm using a UV/VIS spectrophotometer (Lambda XLS+, PerkinElmer, USA).

Results and discussion

Fig.1a and 1b shows the morphologies of pure TiO_2 and Nb_2O_5-TiO_2 nanotube arrays, which were grown in glycerol-H_2O contained NH_4F electrolyte. After 3h anodization, both of tubes are open with the length of 1μm and diameters of around 100 nm. No significant changes are observed in the surface morphology before and after doping since low concentration of Nb in Ti-Nb alloy. This is consistent with result previously grown nanotubes in ethylene glycol contained NH_4F electrolyte.[8] The corresponding XRD patterns of pure TiO_2 and Nb_2O_5-TiO_2 nanotubes annealed at 450°C shown in Fig.1c. As-formed nanotubes can be converted from amorphous to anatase phase with heat-treatment. No clear peaks assigning to Nb_2O_5 were observed due to low concentration. Previous reports have confirmed that Nb exists in the form of Nb_2O_5 after anodization by XPS analysis.[8,13] Inset of Fig.1c is magnified XRD patterns in the range of 2θ=24~27°. It is found that after Nb^{5+} doping the peaks assigned to anatase phase shifts towards higher angles, which suggests the variation of d-spacing due to the occupation of Nb^{5+} ions on TiO_2 matrix.[14]

Fig.2a shows the contact angles of water droplet on pure TiO_2 and Nb_2O_5-TiO_2 nanotube layers calcined at 450°C. Both of the anodic films exhibit surface hydrophilicity. Compared with pure

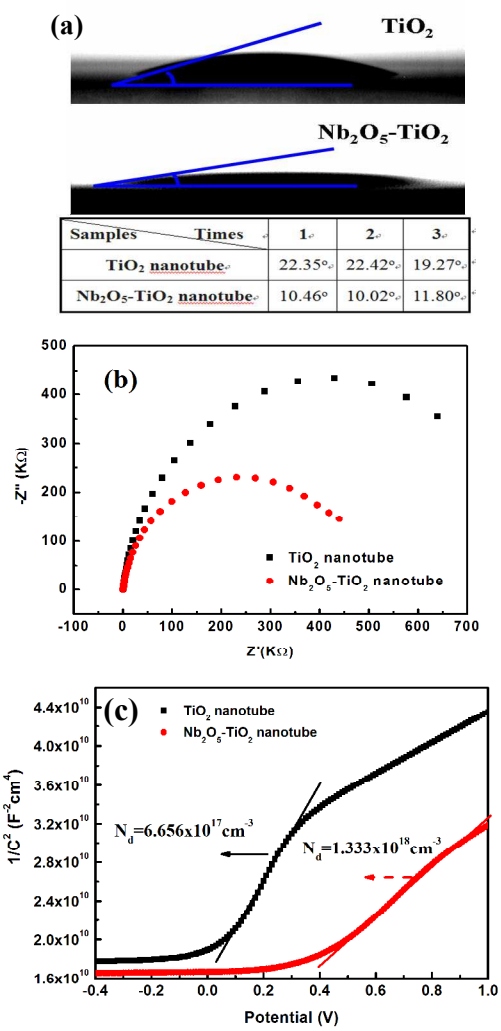

Fig.2 (a) Contact angle images of TiO_2 nanotubes and Nb_2O_5-TiO_2 nanotubes with deionized water droplets. (b) Nyquist plots of pure TiO_2 nanotubes and Nb_2O_5-TiO_2 nanotubes obtained from 0.1 M KCl containing 2.0 mM $Fe(CN)_6^{3-/4-}$electrolyte with an amplitude of 5 mV in frequency range of 0.01~100000 Hz.(c) Mott-Schottky plots of Nb_2O_5-TiO_2 and pure TiO_2 nanotube arrays in 0.5 M Na_2SO_4 electrolyterecorded at frequency of 1 kHz.

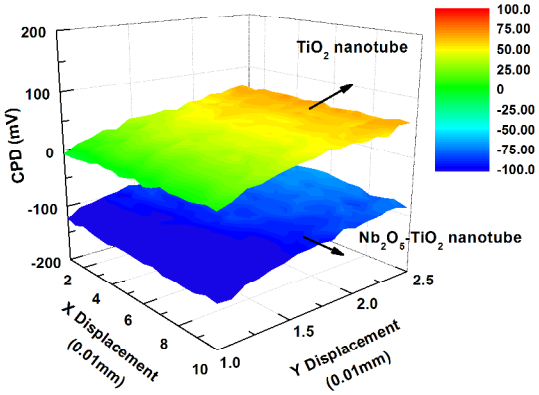

Fig.3 The contact potential differences (CPD) of TiO_2 and Nb_2O_5-TiO_2 nanotubes.

TiO_2 (contact angle of 22.35°), Nb_2O_5 doped TiO_2 nanotube has a smaller contact angle (10.46°), which reveals a more hydrophilic surface and better wettability. Parallel experimental results have shown the same trend as displayed in inset of Fig.2a. Nb^{5+} ion replaces Ti^{4+} in the lattice as an n-type dopant to form hybridized Nb4d-Ti3d states in conduction band [15] after anodization of Ti-Nb alloy. This could bring high oxidation states and a higher proportion of hydroxyl groups on the surface,[16] which leads to an improved wettablility in Nb_2O_5-TiO_2 nanotube. Nyquist impedance plots of TiO_2 and Nb_2O_5-TiO_2 nanotube arrays are shown in Fig.2b. The semicircle diameter represents the charge-transfer resistance (R_{ct}) value for $Fe(CN)_6^{3-/4-}$probe. Obviously, with 450°C heat-treatment a remarkable decrease in the semicircle diameter of Nb_2O_5-TiO_2 nanotube was obtained, which indicated the electron transfer resistance at the electrode/electrolyte interface decreased by Nb doping. In other words, the electrochemical oxidation-reduction reaction rate of $Fe(CN)_6^{3-/4-}$probe on Nb_2O_5-TiO_2 nanotubes is faster than pure TiO_2. To further clarify the Nb_2O_5 doping effect on the band structure, Mott-Schottky (M-S) analysis was performed. According to classical Mott-Schottky theory[17], for n-type semiconductor the charge carrier density can be determined by complex impedance measurements using the following expression:

$$\frac{1}{C^2}=\frac{2}{q\varepsilon\varepsilon_0 N_d A^2}(E-E_{FB}-\frac{kT}{q})$$

Here, C is the differential capacitance of the space-charge region and N_d carrier concentration. ε denotes dielectric constant of semiconductor (ε=41.4 for antase[18]), ε_0 the permittivity of free space (8.854×10^{-12} Fm^{-1}), E applied potential and E_{FB} the flat-band potential. A is surface area of sample ($1cm^2$ for nanotube layers). The quantities q, k and T represent the elementary charge (1.6×10^{-19}C), Boltzmann's constant, and temperature in K, respectively. In Fig.3c, an obvious decrease in the slope in M-S plot is indicative of increasing carrier concentration after Nb_2O_5 doping. Carrier concentrations N_d of Nb_2O_5-TiO_2 nanotube and pure TiO_2 nanotube can be calculated by using extracted slope of the linear regions from Fig.2c as 1.333×10^{18} $cm^{-3}$and 6.656×10^{17} cm^{-3}, respectively.

To further verify Nb_2O_5 doping effects on energy band, the surface work functions of samples were characterized by Kelvin probe measurement.[19] Fig.3 is CPD 3D-distribution maps of pure TiO_2 nanotube and Nb_2O_5-TiO_2 nanotube after 450°C annealing. The data are collected by Au reference probe (surface work function of 5.1eV) with scanning step of 100 μm. It can be seen that due to the surface roughness of both anodic layers CPDs have a slight change in the values of scanning area. Comparing to the pure TiO_2 nanotube, the remarkable decrease of CPD is observed in Nb_2O_5-TiO_2 nanotube. The relationships between surface work function and CPD are shown as follow:

$$CPD=\Phi(sample)-\Phi(Au)=\Phi(sample)-5.1eV$$

where Φ is surface work function. We can calculate the surface work function of pure TiO_2 nanotube and Nb_2O_5-TiO_2 nanotube are approx. 5.15 eV and 5.0 eV, respectively. That is with 0.1wt% Nb doping the apparent feature in energy band is Fermi level moves upward to the conduction band of TiO_2 because of strong hybridization between Ti and Nb. This shift of Fermi level will lead to an increase of carrier concentration in conduction band. Nb doping effects on electric band structure, carrier concentration, and resistivity have been verified by both theoretical calculations and experimental results,[15,20] which are in good agreement with CPD change and our Mott-Schottky results.

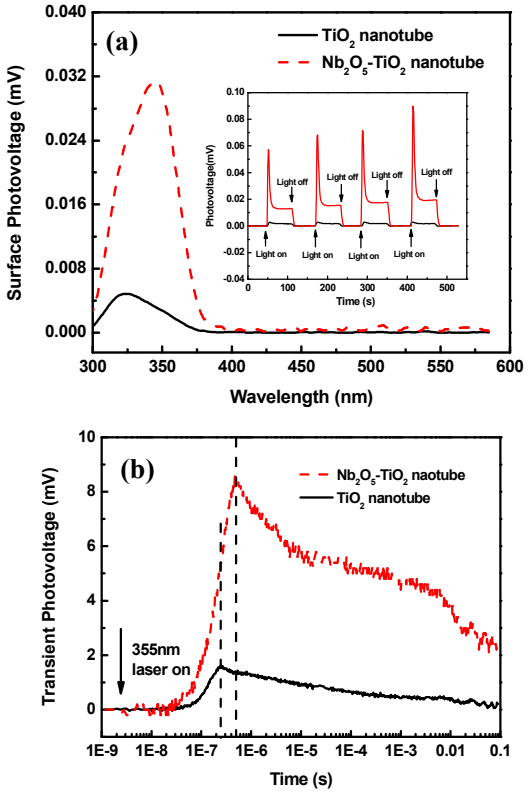

Fig.4 Surface photovoltage spectra (a) and Transient photovoltage responses (b) of TiO_2 and Nb_2O_5-TiO_2 nanotubes. Inset: transient surface photovoltage responses under the illumination of 355 nm.

The charge separation efficiency plays an important role in photocatalytic activity. Here, surface photovoltage spectroscopy (SPS) and transient photovoltage measurement (TPV) were used to investigate the behaviors of photoinduced carriers. When samples are excited by the light with energy larger than band-gap, massive photogenerated carriers are generated and then separated by build-in electric field. That is, photoinduced electrons and holes transfer in opposite directions, resulting in the change of surface band bending and generation of surface photovoltage signals. Fig.4a shows SPS spectra of Nb_2O_5-TiO_2 and TiO_2 nanotube arrays as a function with wavelength. In both cases, the SPV signals give positive responses in the range of 300-400 nm, which indicates under ultraviolet illumination band-to-band transition occurs and photoinduced holes move to the surface. Obviously, 0.1wt% Nb_2O_5 doped TiO_2 nanotube layer shows approx. 6 times higher than pure TiO_2 in the intensity of surface photovoltage response with slight peak red-shift. Since no significant differences in nanotube morphology and thickness are found before or after Nb doping, this increased surface photovoltage signal can be assigned to Nb beneficial effect in

separation and transport of photogenerated carriers in TiO_2 nanotubes. Inset of Fig.4a is photovoltage transients of both nanotube layers under 355 nm illuminations. A clear photovoltage response is generated or vanished with monochromatic light on or off. As apparent, Nb_2O_5-TiO_2 nanotube exhibits considerable strong and stable photovoltage

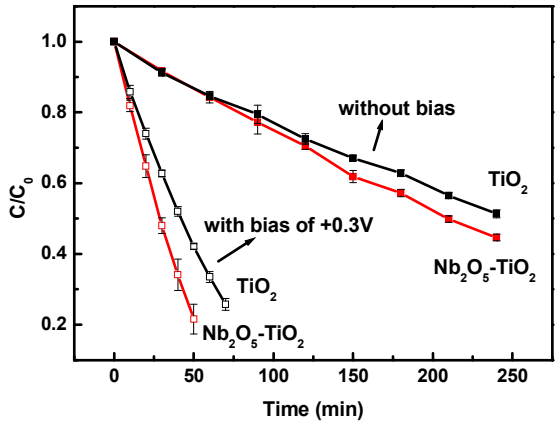

Fig.5 Photocatalytic and photoelectrocatalytic degradations of Acid Orange 7 (AO7, $C_{16}H_{11}N_2O_4SNa$, C_0=15 μM in aqueous solution) on TiO_2 and Nb_2O_5-TiO_2 nanotubes under light of 365 nm.

intensity, which is consistent with the results in Fig.4a. In addition, according to previous report [21] an about 2.5 times higher photocurrent was obtained from Nb_2O_5-TiO_2 nanotubes comparing with non-doped TiO_2 nanotubes. This can further support the improved surface photovoltage intensity. To further understand the kinetics of photo-generated charges transfer by Nb doping effect the TPV measurements were conducted under the illumination of 355 nm laser pulse as shown in Fig.4b. The TPV signals were recorded in the range of 1 ns to 0.1 s. We can obtain the information on the generation, separation, and recombination of photoinduced charges directly. As seen, both of TPV signals show positive values, indicating positive charges transfer to surface.[22] Additionally, higher photoresponse is achieved in Nb_2O_5-TiO_2 nanotube arrays, which means more holes are transferred to surface by Nb doped effect. It is well known TiO_2 has large Maxwell relaxation time,[23] the time of TPV maximum (t_{max}) is affected by lifetime of charge carriers. As expected, t_{max} of Nb_2O_5-TiO_2 nanotube is prolonged to longer timescale than that of pure TiO_2. This demonstrates that trace amount of Nb dopant can suppress the recombination of photogenerated carriers in excited TiO_2 nanotube arrays. It is also worthy to note a shoulder peak appears in the range of 10^{-5}s to 10^{-2}s only in Nb_2O_5-TiO_2 nanotube TPV spectrum. As previous reported, [23,24] this slow process (timescale is longer than 10^{-5}s) can be assigned to diffusion of photogenerated carriers under concentration gradients. Therefore, we can conclude that the Nb dopant promote further separation of electron-hole pairs.

Fig.5 shows the photocatalytic (PC) and photoelectrocatalytic (PEC) activity of TiO_2 and Nb_2O_5-TiO_2 nanotube arrays with error analysis. In PEC measurement the applied bias of +0.3V is chosen to achieve 100% of photogenerated electrons was removed from the conduction band of TiO_2.[25] Clearly, faster degradation efficiency is obtained in PEC process because applied positive bias can effectively promote the photogenerated electrons to the external circuit, and avoid photogenerated electrons recombination with oxidative intermediates. Furthermore, regarding to both of PC and PEC data, Nb_2O_5-TiO_2 nanotube layer exhibits higher degradation efficiency than pure TiO_2. This result is in line with SPV and TPV trend, which suggests the present of Nb_2O_5 in TiO_2 can affect separation of photoinduced carriers.

Conclusions

In summary, Nb_2O_5-TiO_2 nanotube layers were fabricated by electrochemical anodization. The findings in this work have revealed a considerable beneficial effect of small amount (0.1wt%) Nb_2O_5 addition in surface hydrophilic property, charge transfer resistance, and surface energy band structure. In addition, with Nb_2O_5 doping charge separation efficiency of photogenerated carriers is enhanced by the measurements of SPV and TPV, which results in a higher photocatalytic and photoelectrocatalytic activities in TiO_2 nanotubes.

Acknowledgements

For financial support the authors are thankful to the National Natural Science Foundation of China (No.21203043), China Postdoctoral Science Foundation (No.2012M520729 and No.2013T60361), Postdoctoral Research Foundation of Heilongjiang Province (LRB12-008) and Initial Research Funding for talents by Harbin Institute of Technology. The authors would like to acknowledge Prof. Zhonghua Li (Harbin Institute of Technology, China) and Prof. Dejun Wang (Jilin University, China) for technical supports.

Notes and references

[a] *Department of Catalysis Science and Engineering, School of Chemical Engineering and Technology, Harbin Institute of Technology, Harbin, 150001, PR China. Tel: +86 451 86413708; E-mail: yangmin@hit.edu.cn*
[b] *Key Laboratory of Functional Inorganic Material Chemistry (Heilongjiang University), Ministry of Education, Harbin, 150001, PR China.*
[c] *Research Center for Analytical Sciences, Northeastern University, Shenyang, 110004, PR China.*

1 V. Zwilling, E. Darque-Ceretti, A. Boutry-Forveille, D. David, M.Y. Perrin and M. Aucouturier, *Surf. Interface Anal*, 1999, **27,** 629-637.
2 K. Lee, A. Mazare, P. Schmuki, *Chem.Rev.,* 2014, **114**, 9385-9454.
3 I. Paramasivam, H. Jha, N. Liu, P. Schmuki, *Small,* 2012, **8,** 3073-3103.
4 Y.C. Nah, I. Paramasivam, P. Schmuki, *ChemPhysChem*, 2010,**11,** 2698-2713.
5 J.H. Park, S. Kim, A.J. Bard, *Nano Lett.*, 2006, **6(1)**, 24-28.
6 S. Furukawa, Y. Ohno, T. Shishido, K. Teramura, T. Tanaka, *ACS Catal.*, 2011,**1**, 1150-1153.
7 M. Yang, H. Jha, N. Liu, P. Schmuki, *J.Mater.Chem.*, 2011, **21**, 15205-15208.
8 M. Yang, D. Kim, H. Jha, K. Lee, J. Paul, P. Schmuki, *Chem.Commun.*, 2011, **47**, 2032-2034.
9 D. Kurita, S. Ohta, K. Sugiura, H. Ohta, K. Koumoto, *J. Appl. Phys.* 2006, **100**, 096105.
10 H. Cui, K. Dwight, S. Soled, A. Wold, *J.Sol.Stat.Chem.*, 1995,**115**,187-191.

11 X. Wei, T.F. Xie, D. Xu, Q.D. Zhao, S. Pang, D.J. Wang, *Nanotechnology*, 2008, **19**, 275707.

12 Q.D. Zhao, D.J. Wang, L.L. Peng, Y.H. Lin, M.Yang, T.F. Xie, *Chem.Phys.Lett.*, 2007, **434**, 96-100.

13 M.Z. Atashbar, H.T. Sun, B. Gong, W. Wlodarski, R. Lamb, *Thin Solid Films*, 1998, **326**, 238-244.

14 J.T. Park, W.S. Chi, H. Jeon, J. H. Kim, *Nanoscale*, 2014, **6**, 2718-2729.

15 X.D. Liu, E.Y. Jiang, Z.Q. Li, Q.G. Song, *Appl.Phys.Lett.*, 2008, **92**, 252104.

16 I.P. Parkin, R.G. Palgrave, *J.Mater.Chem.*, 2005, **15**, 1689-1695.

17 R. O'Hayre, M. Nanu, J. Schoonman, A. Goossens *J. Phys. Chem. C* 2007, **111**, 4809-4814.

18 J.Y. Kim, H.S. Jung, J.H. No, J.R. Kim, K.S. Hong, *J. Electroceram* 2006, **16,** 447-451.

19 Q.D. Zhao, T.F. Xie, L.L. Peng, Y.H. Lin, P. Wang, L. Peng, D.J. Wang, *J.Phys.Chem. C*, 2007, **111**, 17136-17145.

20 Y. Furubayashi, T. Hitosugi, Y. Yamamoto, K. Inaba, G. Kinoda, Y. Hirose, T. Shimada, T. Hasegawa, *Appl.Phys.Lett.*, 2005, **86**, 252101.

21 C. Das, P. Roy, M. Yang, H. Jha, P. Schmuki, *Nanoscale*, 2011, **3,** 3094-3096.

22 T.F. Jiang, T.F. Xie, L.P. Chen, Z.W. Fu, D.J. Wang, *Nanoscale*, 2013, **5**, 2938-2944.

23 V. Duzhko, V.Y. Timoshenko, F. Koch, T. Dittrich, *Phys.Rev.B*, 2001, **64**, 075204.

24 S. Li, L.J. Zhang, T.F. Jiang, L.P. Chen, Y.H. Lin, D.J. Wang, T.F. Xie, *Chem.Eur.J.*, 2014, **20**, 311-316.

25 X.L. Liu, H.M. Zhang, C. Liu, J.Y. Chen, G.Y. Li, T.C. An, P.K. Wong, H.J. Zhao*, Catal. Today*, 2014, **224***,* 77-82.

Graphical Abstract

Nb_2O_5 doped TiO_2 nanotube arrays were fabricated by electrochemical anodization from Nb-Ti alloy. Nb beneficial effects show on the enhanced surface hydrophilicity, low charge-transfer resistance, and improved separation efficiency of photogenerated charge, which results in higher photocatalytic/photoelectrocatalytic activities.